University of Reading

# *Atmosphere drives recent interannual variability of the Atlantic meridional overturning circulation at 26.5°N*

Article

Supplemental Material

Roberts, C. D., Waters, J., Peterson, K. A., Palmer, M., McCarthy, G. D., Frajka-Williams, E., Haines, K. ORCID: https://orcid.org/0000-0003-2768-2374, Lea, D. J., Martin, M. J., Storkey, D., Blockey, E. W. and Zuo, H. (2013) Atmosphere drives recent interannual variability of the Atlantic meridional overturning circulation at 26.5°N. Geophysical Research Letters, 40 (19). pp. 5164-5170. ISSN 0094-8276 doi: https://doi.org/10.1002/grl.50930 Available at https://centaur.reading.ac.uk/34301/

It is advisable to refer to the publisher's version if you intend to cite from the work. See Guidance on citing.

To link to this article DOI: http://dx.doi.org/10.1002/grl.50930

Publisher: American Geophysical Union

All outputs in CentAUR are protected by Intellectual Property Rights law, including copyright law. Copyright and IPR is retained by the creators or other copyright holders. Terms and conditions for use of this material are defined in the End User Agreement.

University of Reading

www.reading.ac.uk/centaur

**CentAUR**

Central Archive at the University of Reading

Reading's research outputs online

# Auxiliary material for 'Atmosphere drives recent interannual variability of the Atlantic meridional overturning circulation at 26.5°N'

C.D. Roberts,[1] J. Waters,[2] K.A. Peterson,[1] M.D. Palmer,[1] G.D. McCarthy,[3] E. Frajka-Williams,[4] K. Haines,[5] D.J. Lea,[2] M.J. Martin,[2] D. Storkey,[2] E.W. Blockley,[2] H. Zuo,[6]

Corresponding author: C. D. Roberts, Met Office Hadley Centre, Fitzroy Road, Exeter, EX1 3PB, UK. (chris.roberts@metoffice.gov.uk)

[1]Met Office Hadley Centre, Exeter, UK.

## 1. Auxiliary methods

### 1.1. FOAM-3DVAR description

The version of FOAM-3DVAR we have used is based on v3.2 of the NEMO global ocean model [*Madec*, 2008] configured with 75 vertical z-levels and a horizontal resolution of $\sim 0.25^{\circ}$ coupled to the CICE v4.1 sea-ice model [*Hunke and Lipscomb*, 2010]. Changes to the physical model compared to the previous version of FOAM [*Martin et al.*, 2007; *Storkey et al.*, 2010] include an update to the TKE scheme for vertical mixing, geographical variation of the parameters used to calculate bottom friction, inclusion of a bottom boundary layer scheme, and the addition of a parameterization for tidal mixing. Surface

[2]Met Office, Exeter, UK.

[3]National Oceanography Centre,
Southampton, UK.

[4]Department of Ocean and Earth Science,
University of Southampton, Southampton,
UK.

[5]Department of Meteorology, University
of Reading, Reading, UK.

[6]European Centre for Medium-Range
Weather Forecasts, Reading, UK.

boundary conditions are provided as 3-hourly fields of 10 m winds, 2 m air temperature, 2 m specific humidity, short/long wave radiation, precipitation, and snowfall from the ERA-interim atmosphere reanalysis [*Dee et al.*, 2011]. Turbulent air-sea surface fluxes are calculated using the bulk formulae of *Large and Yeager* [2004].

Data assimilation of sub-surface temperature profiles, sub-surface salinity profiles, sea-surface temperatures, sea surface height (SSH) and sea-ice concentrations is performed using an incremental 3D-VAR data assimilation system, NEMOVAR [*Waters et al.*, 2013]. The scheme is run in a First-Guess-at-Appropriate-Time (FGAT) framework with a 24 hour assimilation window and the model is initialized with the data assimilation increments using the Incremental Analysis Update (IAU) scheme of *Bloom et al.* [1996]. The NEMOVAR system includes multivariate assimilation of temperature, salinity, SSH and velocities, with balance relationships preserving the T-S relationship in density plus hydrographic and geostrophic balance [*Weaver et al.*, 2005]. Furthermore, bias correction schemes are implemented to reduce the bias inherent in satellite measurements of SST [*Donlon et al.*, 2012; *Martin et al.*, 2007] and to reduce the bias in the (supplied) mean dynamic topography required to convert measurements of sea level anomaly into sea surface height [*Lea et al.*, 2008]. In addition, a weak (-33.3 mm/day/psu) Haney retroaction term is prescribed to damp anomalies in sea-surface salinity, along with a 1 year timescale damping of 3-dimensional temperature and salinity to seasonally varying climatological values. These terms are included to restrict drift in the weakly constrained surface salinity and abyssal ocean, but additional sensitivity experiments reveal that they have a negligible impact on the simulation of the AMOC at 26.5°N (auxiliary figure 5).

### 1.2. Calculation of the AMOC in model simulations

To observe the AMOC at 26.5°N, the RAPID array combines measurements of the Gulf Stream through the Florida Straits, Ekman transports calculated from zonal wind-stress, western boundary transports measured using current meters, geostrophic transports measured with dynamic height moorings in the ocean interior, and a mass-compensation term to ensure that there is zero net transport through the section [*Rayner et al.*, 2011]. In order to make the most appropriate comparisons, all model transports are calculated using an analogous 'RAPID-style' methodology.

Velocities in the Florida Straits and the 'western boundary wedge' (WBW) are specified to be the same as model velocities. In the RAPID array, the WBW is the region west of 76.75°W (except during 2005/06 when the region was expanded to west of 76.5°W due to the collapse of a boundary mooring). In the model, the WBW is defined as the region west of 76.25°W. The model region is expanded by an additional two ∼0.25° grid-points to ensure that the simulated western boundary current is contained within the model WBW. Ekman velocities are calculated from zonal wind-stress as

$$v_{ek} = \frac{-1}{f\rho_0 A_{ek}} \int_w^e \tau_x \, dx,$$

where $A_{ek}$ is the cross-sectional area of the Ekman layer (assuming a depth of 100 m), $\tau_x$ is the zonal wind-stress, and $\rho_0$ is a reference density. East of 76.25°W, geostrophic velocities ($v_{geo}$) are calculated using

$$v_{geo} = \frac{-g}{f}\frac{\partial D}{\partial x},$$

$$D = \int_{z_{ref}}^{z} \frac{\sigma}{\rho_{ref}} \, dz,$$

where $g$ is acceleration due to gravity, $f$ is the Coriolis parameter at 26.5°N, $D$ is dynamic height relative to a reference depth, $\sigma$ is an *in situ* density anomaly, and $\rho_{ref}$ is a reference *in situ* density. When calculating dynamic heights, we use a reference depth of 4740 m (the same depth as used in the RAPID calculations) or the ocean bottom. Finally, a mass-compensation term is applied as a uniform velocity added to the geostrophic velocity field that ensures zero net-flow across the section. Overturning stream functions ($\Psi$) are then defined as

$$\Psi = \int_{z=0}^{z} \int_{w}^{e} v \, dx \, dz.$$

### 1.3. Statistical methods

To evaluate the significance of differences in correlations calculated from model data and observations across different experiments, we use the following bootstrap method. For each variable, we generate 10,000 realizations of the observed time series by drawing data randomly (with replacement) from the 81 available months between Apr 2004 and Dec 2010. Corresponding model time series are created using exactly the same randomly selected dates. These samples are used to calculate the variability of correlation coefficients associated with month-to-month differences in the agreement between observed and simulated anomalies. The resulting distribution of differences in correlations is used to calculate probabilities for the following hypotheses:

$$H0 : r_1 = r_2$$

$$H1 : r_1 > r_2$$

For probabilities less than 0.05, we reject the null hypothesis that correlations are equal. We use this method because statistics derived from Fisher r-to-Z transformations do not give accurate results when data are not independent (in this case, each pair of correlations is calculated using the same observational data). Our conclusions do not change if we use probabilities calculated using the Steiger Z transform for comparing elements of a correlation matrix [*Steiger*, 1980].

### 1.4. RAPID sensitivity calculations

RAPID calculations combine transports in the Florida Straits, the Ekman layer and west of 76.75°W (referred to as the western boundary wedge) with geostrophic transports ($\mathrm{Td}_{int}$) relative to a reference level that is adjusted such that mass is conserved across the section:

$$\int [Td_{flo}(z) + Td_{ek}(z) + Td_{wbw}(z) + Td_{int}(z) + Td_{ext}(z)]dz = 0$$

where the first three terms are the Florida Straits, Ekman and western boundary wedge transport. The compensated geostrophic transport is expressed in the final two terms. This may be written as

$$Td_{int}(z) + Td_{ext}(z) = \frac{-g\Delta D_{ref}(z)}{f} + v_{comp,ref}.w(z)$$

where $\Delta$D is the dynamic height difference across the basin relative to the reference level, $f$ is the Coriolis parameter, $v_{comp,ref}$ is the compensation velocity applied at the reference level and w(z) is the width of the basin.

It is necessary that w(z) reflects the narrowing basin, particularly below the depth of the mid-Atlantic ridge at 3200 m, lest too much flow results in the deep ocean. However,

due to this variation in the width of the basin, the resultant deep flow is sensitive to the reference level chosen.

Consider the examples in auxiliary figure 2. The reference level of 4740 m is the reference level used in RAPID calculations and the associated $\mathrm{Td}_{int}$ is shown by the black solid line. It is chosen as an approximate depth above which North Atlantic deep water flows south and below which Antarctic bottom water flows north. The $\mathrm{Td}_{ext}$ that needs to be added to this transport profile to conserve mass is small (black, dashed). On the other hand, if the reference level of 1780 m is chosen, a much larger $\mathrm{Td}_{ext}$ is necessary. This is because a reference level of 1780 m is almost at the maximum of the southward flow of upper North Atlantic deep water and a large velocity needs to be added to recover this southward flow. It has the additional consequence of reducing the flow in the deep ocean where the width of the basin reduces to zero.

The resulting stream functions from reference levels of 4740 m and 1780 m are shown in auxiliary figure 3 (black-solid and black-dashed, respectively). All stream functions resulting from varying the reference level between 1090 m and 4740 m are contained in the gray envelope.

RAPID calculations choose 4740 m as a reference level as it is the depth where zonally integrated-transport from hydrographic sections is near-zero, results in a conservative application of the mass conservation constraint, and it allows comparison with bottom pressure records at the western boundary [*McCarthy et al.*, 2012]. While there is some variation in the shape of the overturning at depth due to choice of reference level, the

resultant value of the strength of the AMOC is consistent within 2 Sv, the accuracy of the calculation [*Cunningham et al.*, 2007].

## References


Bloom, S., L. Takacs, A. Da Silva, and D. Ledvina (1996), Data assimilation using incremental analysis updates, *Monthly Weather Review*, *124*(6), 1256–1271.

Cunningham, S., et al. (2007), Temporal variability of the Atlantic meridional overturning circulation at 26.5°N, *Science*, *317*(5840), 935–938.

Dee, D., et al. (2011), The ERA-Interim reanalysis: Configuration and performance of the data assimilation system, *Quarterly Journal of the Royal Meteorological Society*, *137*(656), 553–597.

Donlon, C. J., M. Martin, J. Stark, J. Roberts-Jones, E. Fiedler, and W. Wimmer (2012), The operational sea surface temperature and sea ice analysis (OSTIA) system, *Remote Sensing of Environment*, *116*, 140–158.

Hunke, E., and W. Lipscomb (2010), *CICE: The Los Alamos sea ice model documentation and software users manual version 4.1.*, Los Alamos National Laboratory.

Large, W. G., and S. G. Yeager (2004), *Diurnal to decadal global forcing for ocean and sea-ice models: the data sets and flux climatologies*, National Center for Atmospheric Research.

Lea, D., J.-P. Drecourt, K. Haines, and M. Martin (2008), Ocean altimeter assimilation with observational-and model-bias correction, *Quarterly Journal of the Royal Meteorological Society*, *134*(636), 1761–1774.

Madec, G. (2008), *NEMO ocean engine*, Institut Pierre-Simon Laplace (IPSL).

Martin, M., A. Hines, and M. Bell (2007), Data assimilation in the FOAM operational short-range ocean forecasting system: a description of the scheme and its impact, *Quar-*

*terly Journal of the Royal Meteorological Society*, *133*(625), 981–995.

McCarthy, G. D., et al. (2012), Observed interannual variability of the Atlantic meridional overturning circulation at 26.5°N, *Geophysical Research Letters*, p. doi:10.1029/2012GL052933.

Rayner, D., et al. (2011), Monitoring the Atlantic meridional overturning circulation, *Deep Sea Research Part II: Topical Studies in Oceanography*, *58*(17), 1744–1753.

Steiger, J. H. (1980), Tests for comparing elements of a correlation matrix, *Psychological Bulletin*, *87*(2), 245–251.

Storkey, D., et al. (2010), Forecasting the ocean state using NEMO: The new FOAM system, *Journal of Operational Oceanography*, *3*(1), 3–15.

Waters, J., D. Lea, D. Martin, M. Storkey, and J. While (2013), Describing the development of the new FOAM-NEMOVAR system in the global 1/4 degree configuration, *Forecasting Research Technical Report 578*, Met Office, Exeter, UK.

Weaver, A., C. Deltel, E. Machu, S. Ricci, and N. Daget (2005), A multivariate balance operator for variational ocean data assimilation, *Quarterly Journal of the Royal Meteorological Society*, *131*(613), 3605–3625.

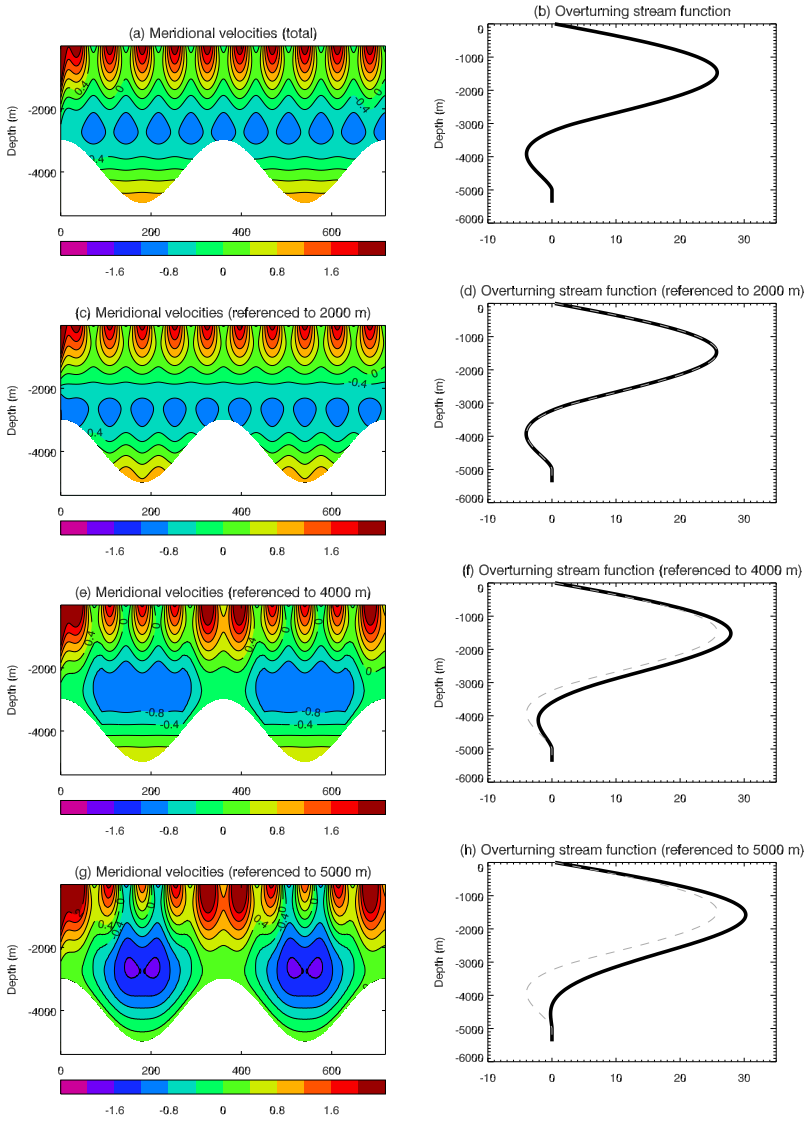


**Figure 1.** Idealized meridional velocity sections and associated overturning stream function profiles showing the impact of different reference levels on the resulting overturning profiles. Dashed gray lines in (d), (f) and (g) correspond to the profile from (b).

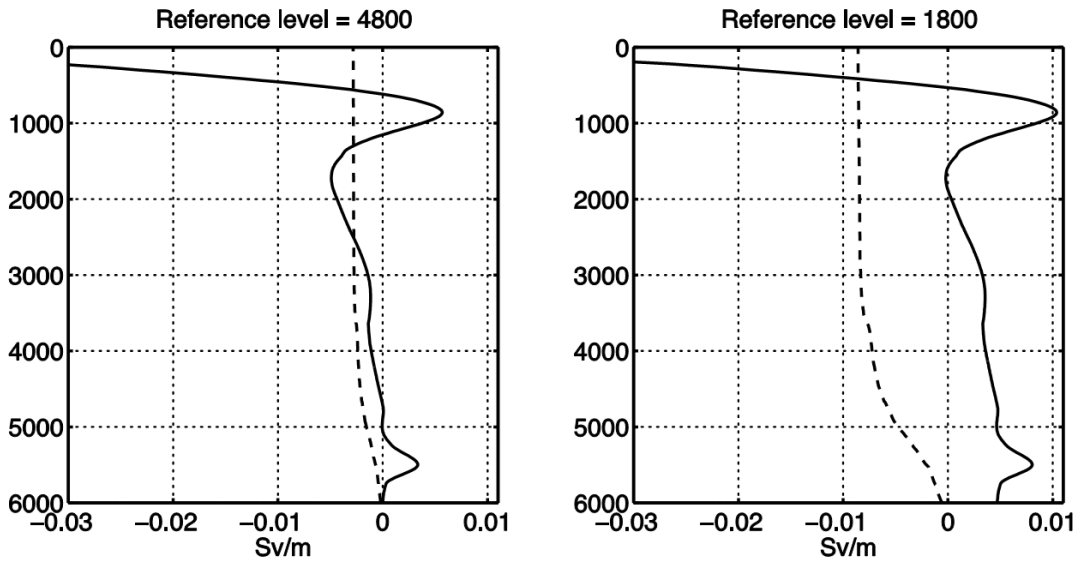


**Figure 2.** Internal transports ($\mathrm{Td}_{int}$; black, solid) for two reference levels and associated compensation profiles ($\mathrm{Td}_{ext}$; black, dashed). The different reference levels result in an offset between the internal transports, which then require different compensation adjustments to satisfy mass-balance across the section. To account for variations in the basin width with depth, the compensation profiles have a vertical structure that affects the shape of the resulting overturning profile.

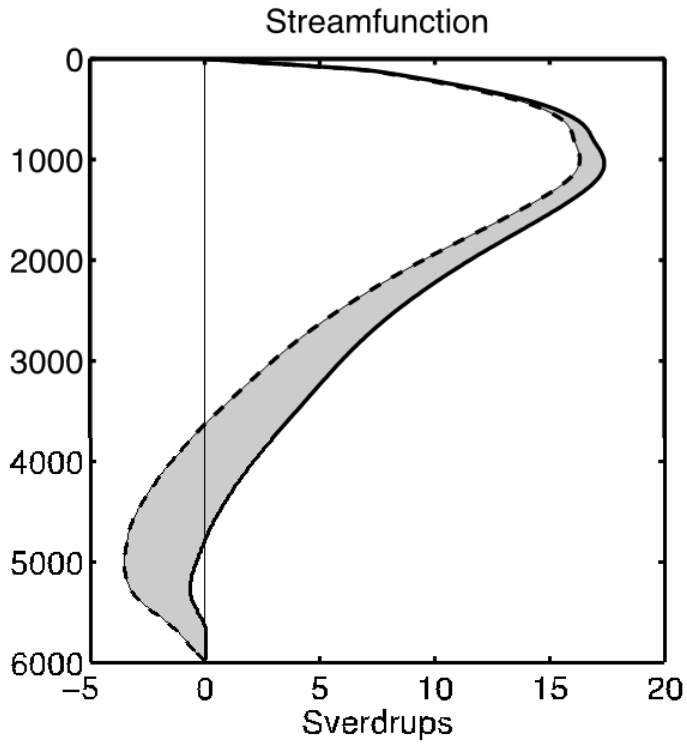


**Figure 3.** Stream functions resulting from the variation of reference level between 1100 dbar and 4800 dbar are represented by the gray area. Two particular reference levels are highlighted: 1800 dbar (black, dashed) and 4800 dbar (black, solid).

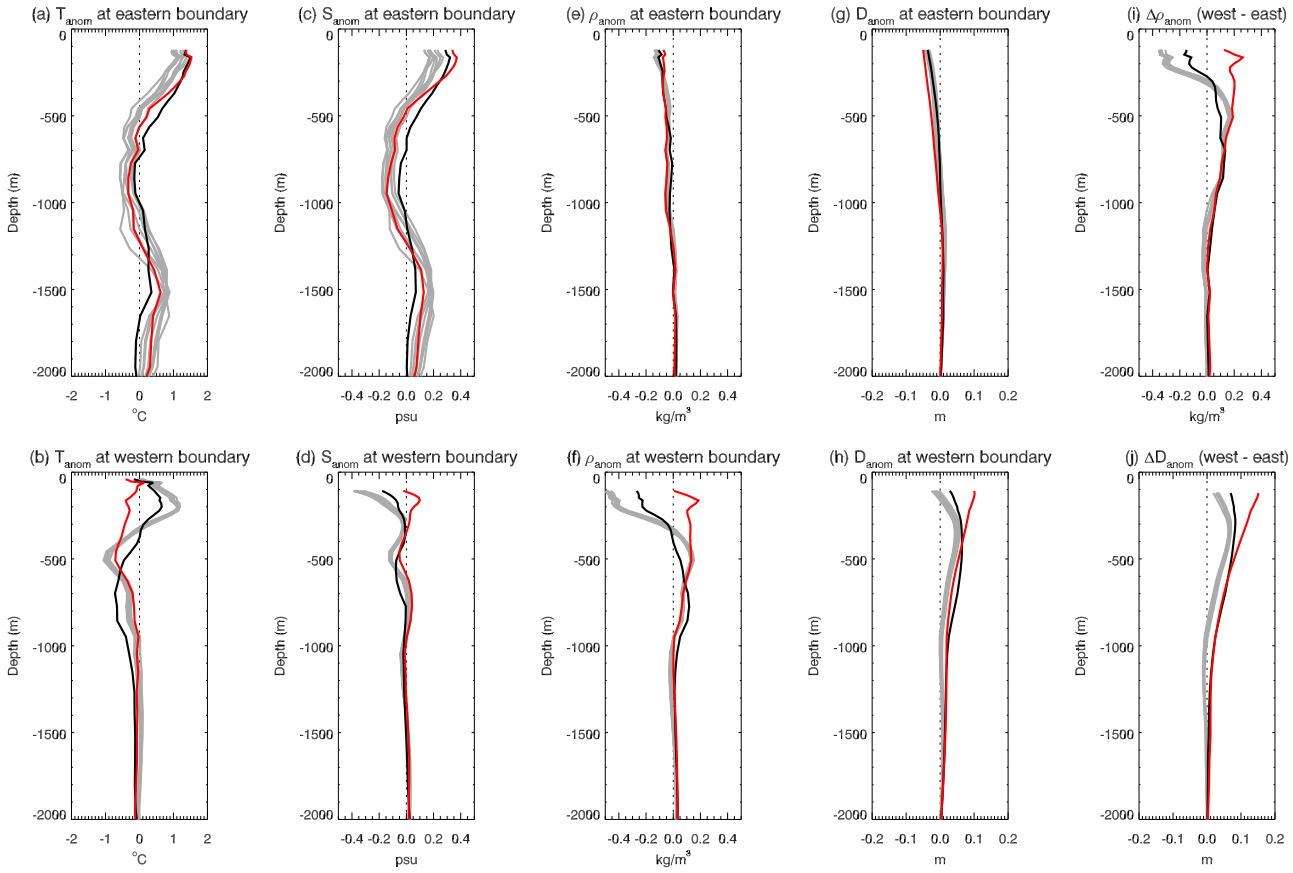


**Figure 4.** Anomalies of (a-b) temperature, (c-d) salinity), (e-f) *in situ* density, and (g-h) dynamic height referenced to 2000 m at the eastern and western boundaries of the North Atlantic at 26.5°N in ASSIM-3DVAR (red), ASSIM-AC (black) and NO-ASSIM (gray lines). Also shown are anomalies in 'west minus east' differences of (i) *in situ* density and (j) dynamic height. Model data are extracted from grid-cells adjacent to the eastern and western Atlantic Ocean boundaries between 24°W - 10°W and 77.5°W - 70°W, respectively. Anomalies are calculated relative to the merged eastern and western boundary profiles provided by the RAPID array. Anomalies are averages calculated using monthly data for the period 01/04/2004 - 31/12/2010.

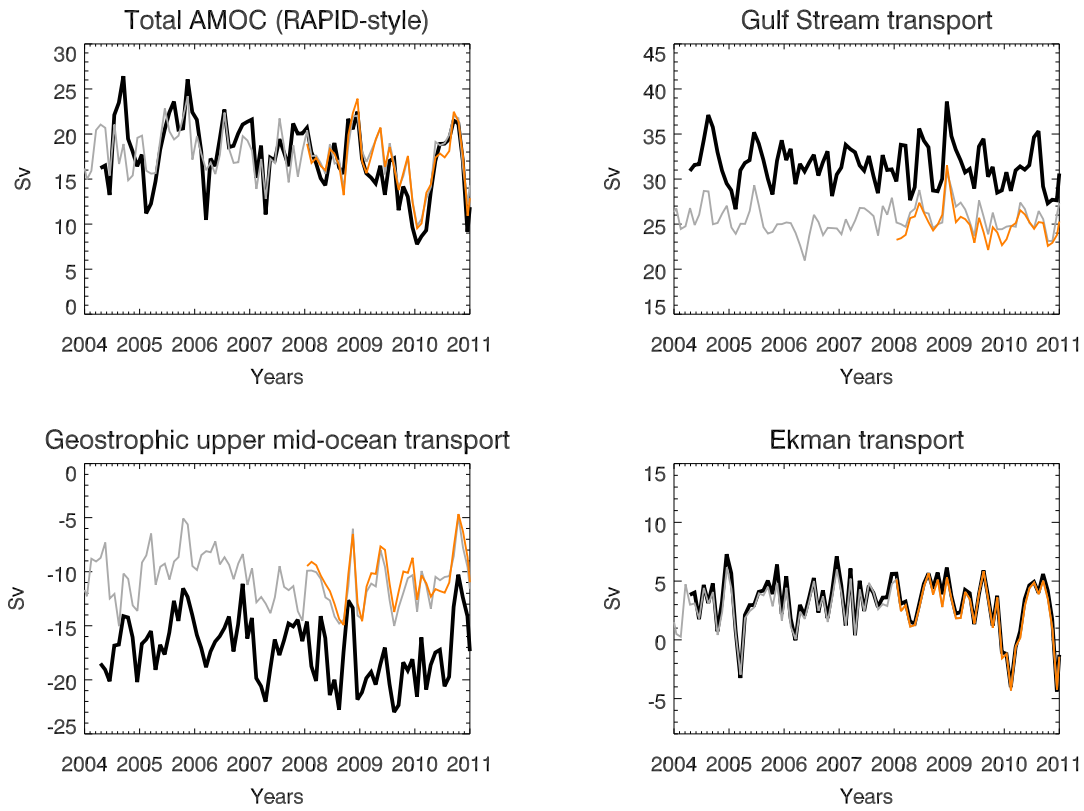


**Figure 5.** Monthly mean time series of components of the AMOC from ASSIM-3DVAR (gray), RAPID observations (black), and a version of ASSIM-3DVAR with all restoring terms disabled (orange).